Open Research Online

The Open University's repository of research publications
and other research outputs

Graphene-based ultrathin flat lenses

Journal Item

How to cite:

Kong, Xiang-Tian; Khan, Ammar A.; Kidambi, Piran R.; Deng, Sunan; Yetisen, Ali K.; Dlubak, Bruno; Hiralal, Pritesh; Montelongo, Yunuen; Bowen, James; Xavier, Stéphane; Jiang, Kyle; Amaratunga, Gehan A. J.; Hofmann, Stephan; Wilkinson, Timothy D.; Dai, Qing and Butt, Haider (2015). Graphene-based ultrathin flat lenses. ACS Photonics, 2(2) pp. 200–207.

For guidance on citations see FAQs.

© 2015 American Chemical Society

https://creativecommons.org/licenses/by-nc-nd/4.0/

Version: Accepted Manuscript

Link(s) to article on publisher's website:
http://dx.doi.org/doi:10.1021/ph500197j

Copyright and Moral Rights for the articles on this site are retained by the individual authors and/or other copyright owners. For more information on Open Research Online's data policy on reuse of materials please consult the policies page.

oro.open.ac.uk

Graphene-Based Ultra-Thin Flat Lenses

Xiang-Tian Kong[1,#], Ammar A. Khan[2,#], Piran R. Kidambi[2,#], Sunan Deng[3,#], Bruno Dlubak[4], Pritesh Hiralal[2], Yunuen Montelongo[2], James Bowen[5], Stéphane Xavier[4], Kyle Jiang[3], Gehan A. J. Amaratunga[2], Stephan Hofmann[2], Timothy D. Wilkinson[2], Qing Dai[1,*], Haider Butt[3,*]

[1]National Center for Nanoscience and Technology, Beijing 100190, China
[2]Electrical Engineering Division, Department of Engineering, University of Cambridge, Cambridge CB3 0FA, UK
[3]School Mechanical Engineering, University of Birmingham, Birmingham B15 2TT, UK
[4]Thales Research and Technology, 91767 Palaiseau, France
[5]School Chemical Engineering, University of Birmingham, Birmingham B15 2TT, UK

*Email: daiq@nanoctr.cn, Tel: +86 10 82545720.
*Email: h.butt@bham.ac.uk, Tel: +44 121 4158623

KEYWORDS Graphene, thin lenses, Fresnel zone plates

ABSTRACT: Flat lenses when compared to curved surface lenses have the advantages of being aberration free and they offer a compact design necessary for a myriad of electro-optical applications. In this paper we present flat and ultra-thin lenses based on graphene, the world's thinnest known material. Monolayers and low number multilayers of graphene were fabricated into Fresnel zones to produce Fresnel zone plates which utilize the absorption properties of graphene for their operation. The working of the lens and their performance in the visible and terahertz regimes was analyzed computationally. Experimental measurements were also performed to characterize the lens in the visible regime and a good agreement was obtained with the simulations. The work demonstrates the principle of atom thick graphene-based lenses, with perspectives for ultra-compact integration.

Fresnel zone plates are diffractive optical elements capable of focusing light. Unlike curved lenses, Fresnel zone plates are based in diffractive rings that deform the field.[1] When the rings are properly design it is possible to produce constructive interference at a given focal point. Binary intensity Fresnel zone plates use a flat surface with a set of radially symmetric rings, which alternate between opaque and transparent.[2] Fresnel zone plate offers the possibility of designing high numerical aperture (NA) lens with low weight and small volume. It is hence, widely used in silicon based electronics with various applications, such as optical interconnects,[3] integrated optics,[4] beam focusing[5, 6] and maskless lithography systems.[7]

In this paper we demonstrate Fresnel zone plates (FZP) based lenses made by graphene. Each graphene FZP lens has twenty four zones, with a radius of about 50 μm. This is a major achievement in realizing efficient ultrathin lenses, which has the potential to improve the capabilities of compact optical systems, such as laser focusing for optical storage and fibre-optic communication.

A thin lens is defined as one with a thickness that is negligible compared to the focal length of the lens. Currently, lenses are not thin or flat enough to remove distortions, which limit imaging. Previously aberration was corrected by techniques such as aspheric shapes or multilens designs, resulting in heavy weight and extra space. Hence, it is very important to develop ultrathin lenses and FZPs offers a suitable solution. From the theoretical perspective a diffractive element like FZPs can achieve efficiencies close to 100% with diffraction limited performance[8, 9]. However, the physical constrains limits these possibilities. For instance, the relief of the diffractive plane is one of the sources of multiple aberrations in the focal plane.[10] Therefore, thin diffraction elements are desirable for the reduction of such distortions.

The ultrathin lens based on 60 nm thick gold metasurface, fabricated by Federico Capasso *et al*.,[11] is considered to be a milestone to revolutionise consumer technology form factor. Here we report on the development of an ultrathin FZP lens using graphene on glass with a few nanometers thickness. Graphene is a single two-dimensional (2D) layer of carbon,[12] exhibiting an unique set of opto-electronic properties, in particular high optical transparency, low reflectance and a high carrier mobility at room temperature.[13, 14] This enables multiple functions of signal emitting, transmitting, modulating, and detection to be realized in one material[15] and makes graphene a promising choice for optoelectronic devices.[16] In the visible regime, the optical transmittance of single layer graphene is frequency-independent and solely determined by the fine structure constant $\alpha=e^2/\hbar c$ (c is the speed of light): $T \equiv \left(1+\frac{2\pi G}{c}\right)^{-2} \approx 1-\pi\alpha \approx 0.977$, in which G is universal conductivity of graphene[17]. Compared with the transmittance, the reflectance of graphene under normal light incidence is relatively weak with $R = 0.25\pi^2\alpha^2 T = 1.3\times10^{-4}$.

However, the opacity of multi-layer graphene will increase linearly with the number of layers, *N*, ($T \cong 1-N\pi\alpha$). Unlike single-layer graphene, according to Skulason *et al.,*[18] few-layer graphene could have very high reflection contrast, indicating the possibility of making FZP lens of graphene on glasses. For the FZP based lenses the focal length *f* of the lens is related to the radii *r* of successive zone edges. By means of an approximation for large focal lengths, the radius of the rings can satisfy the equation : $\frac{f}{r_n} = \frac{r_n}{n\lambda}$ (λ is the wavelength of light, n=1, 2, 3…), and radius of the *n*th zone (r_n) in a FZP lens $r_n = n{r_1}^2$.[19] Setting the focal length to 120 μm at an optical wavelength of 850 nm, the spacing and widths of the Fresnel zones were calculated with different *n*. Figure 1 shows the three-dimensional (3D) schematic diagram of the FZP geometry and its operation. The radius of the central zones was 10 μm and the lens radius of about 49 μm.

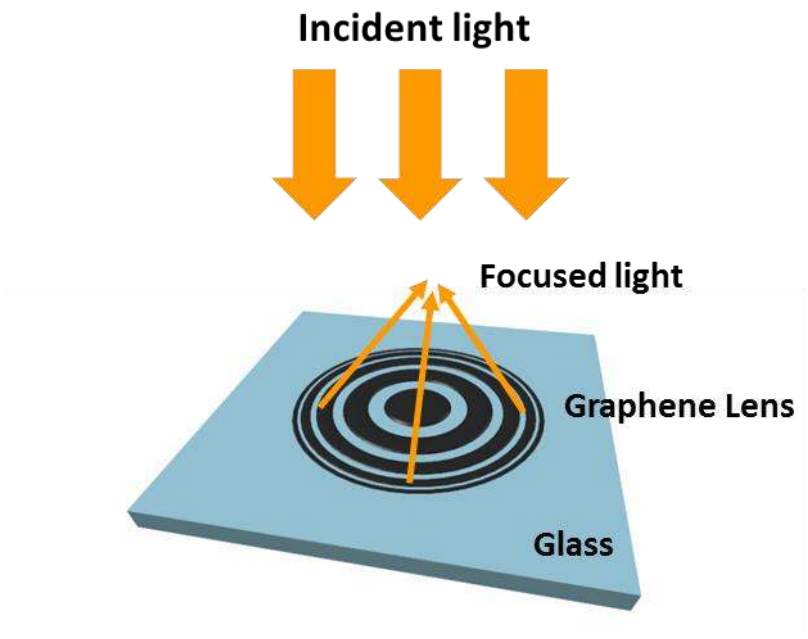

Figure 1. Schematic showing the geometry and reflection mode operation of the graphene Fresnel zone plate, incident light from the top.

The graphene FZP was simulated by finite element method, in which the lens is illuminated perpendicularly by a Gaussian beam with a waist radius of 35 nm. The graphene is modelled as a material whose equivalent permittivity is given by $\varepsilon_g = i\sigma/\varepsilon_0\omega t_g$,[20] where ε_0 is the vacuum permittivity, ω is the angular frequency of light, t_g = 0.335 nm is the monolayer graphene thickness and σ is the optical conductivity of graphene obtained from the Kubo formula.[21] In the Kubo formula, the conductivity is a function of the angular frequency ω, the Fermi level relative to the Dirac point E_F, the relaxation time τ and temperature T_{em}. The relaxation time is obtained from $\tau = \mu E_F/ev_F^2$, where μ = 3000 $cm^2/(Vs)$[22] is the measured dc mobility, e is the electron charge and $v_F = 1 \times 10^6$ m/s is the Fermi velocity. The temperature is assumed to be 300 K. Note that the optical responses of graphene are not influenced by the sign of Fermi level (*p*-doped or *n*-doped), owing to the linear electron dispersion relation of graphene. The thickness of the *N*-layer graphene is set to be equal to Nt_g in the simulations. The optical constant of the glass substrate is cited from Palik[23]. To obtain the electromagnetic field of the reflected light from the lens, the incident field is subtracted from the computed total field. Then, the power flow can be calculated according to the Poynting theorem.

Figure 2(a) shows the computed power flow distribution of the reflected light by the FZP made by 5-layer graphene, illuminated by light with 850-nm wavelength. The radius of the innermost graphene zone is 10 □m. Accordingly, the focal length is equal to 117.6 □m. The horizontal and vertical cross-sectional lines at the focal point are shown in Figures 2(b) and (c) (solid lines), respectively. Here the Fermi level is assumed to be 0.1 eV. This simulation confirms the focusing of the reflected light of the graphene-based lens. The lensing effect relies mainly on the number of layers of graphene for the incident light in the visible and near infrared frequency range. For example, the dashed lines in Figures 2(b) and (c) show the cross sectional lines corresponding to a lens composed of 10-layer graphene. As shown, the power flow at the focal point increases two-fold when the layer number increases from 5 to 10, owing to the increased light absorption.

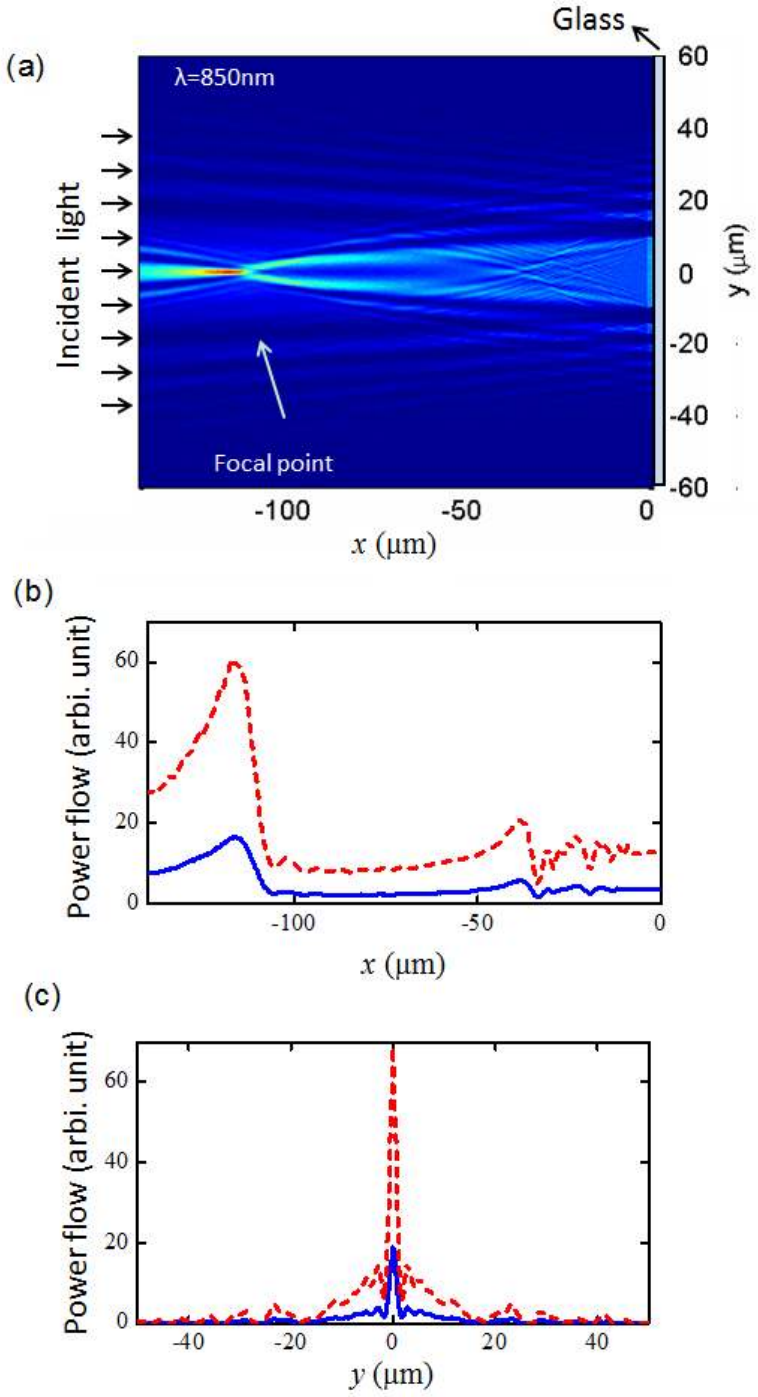

Figure 2. (a) Power flow distribution of the reflected light of the Fresnel zone plate composed of 5-layer graphene. The lenses are located at x = 0 on glass substrate (x> 0). Light illumination of 850-nm wavelength is launched from the leftmost boundaries of the computation domains. (b) Power flow in terms of x extracted at y = 0. (c) Power flow in terms of y at the focal plane (f = 117.65 μm). In (b) and (c), solid and dashed lines correspond with lens with 5- and 10-layer graphene, respectively.

Note that in the visible the absorption of graphene, which is caused by direct interband transitions, is nearly a constant with the Fermi level and charge mobility due to Pauli blocking. The power flow at the focal point almost remains unchanged with varying the Fermi level of graphene. As shown in table 1, that at the Fermi level of 0.1 eV

the power flow at the focal point of the 5-layer graphene lens was approximately equal to 19.1 a.u. When the Fermi level was increased to 0.5 eV, the power flow was 18.8 a.u. Table 1 presents the focal intensities under Fermi level ranging from 0.05 eV to 0.6 eV.

Table 1. Change in the focal intensity of the lens with the Fermi level[1].

Fermi level (eV)	Focal intensity (arbi. unit)
0.05	19.1344
0.1	19.1317
0.2	19.1125
0.3	19.0623
0.4	18.9713
0.5	18.8689
0.6	19.0309

The effect of charge mobility was also studied through simulations. The charge mobility μ has negligibly small influence on the focused intensity distribution of the Fresnel zone plate in a broad range of 100 ~ 10,000 $cm^2/(Vs)$. Figure 3 shows the focused intensity plots across half of the focal plane. The other half is expected to be the same due to the symmetry of the focal point. With the charge mobility increasing from 100 to 10,000 $cm^2/(Vs)$ no change in the focused intensity of 19.1 a.u was observed. Thus, the field distribution of the focused visible light is only negligibly influenced by the Fermi level (*esp.* for $|E_F| < 0.6$ eV) as well as the charge mobility (for μ ranging from 10^2 to 10^4 $cm^2/(Vs)$).

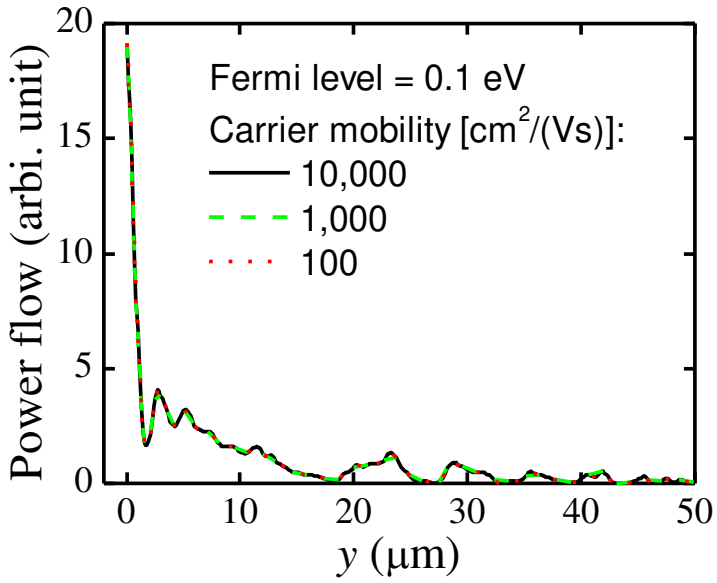

Figure 3. Power flow in terms of *y* at the focal plane with Fermi level of 0.1 eV and carrier mobility of 10,000 $cm^2/(Vs)$ (black solid), 1,000 $cm^2/(Vs)$ (green dashed), 100 $cm^2/(Vs)$ (red dotted), for Fresnel zone plate lens made of 5-layer graphene under illumination of 850-nm wavelength.

Based on the simulation results mono[22, 24] and multi-layer graphene[25, 26] were synthesized by chemical vapour deposition (CVD) and Fresnel zone plates were fabricated by photolithography methods. The as-fabricated graphene lens array was characterized under an optical microscope. Figure 4(a) shows the lens array under the microscope,

[1] with mobility μ equal to 3000 $cm^2/(Vs)$ for lens with 5-layer graphene under illumination of 850 nm wavelength

while Figure 4(b) showing the lens array focusing the light with excellent contrast. Figure 4(c) and (d) demonstrate the magnified version of a single graphene FZP lens and focal point along with the light intensity profile across the horizontal direction. It was clear from the intensity profiles that the focal point exhibits a good contrast. The efficiency of the lens is 6.57%, which is calculated from the ratio of light intensity at the focal point to the total light intensity falling on lenslet. The maximum efficiency reported for the ultrathin lens based on 60 nm thick gold metasurface is approximately 1% for wavelength of 1550 nm.[11] Also designing such metasurface lenses for the visible range will be a challenge due to the fine nanoscaled structures required. The graphene based lenses offer more compactness, lower losses, are much easier to fabricate and also offer tunability in the infra-red range.

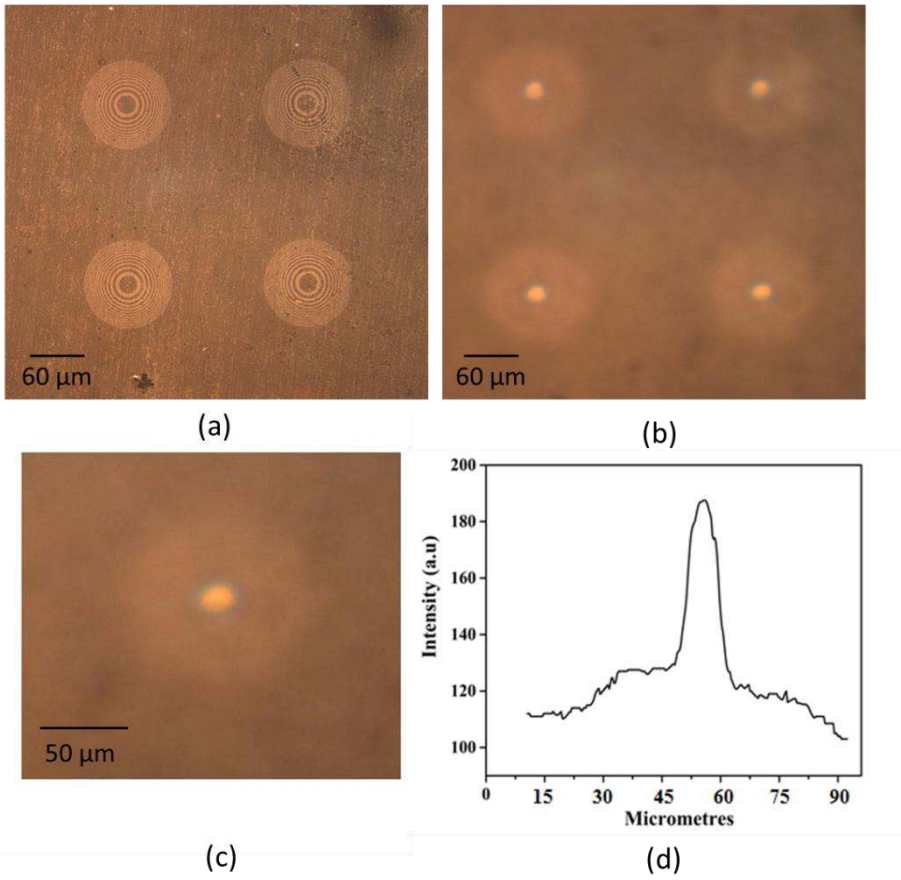

Figure 4. Graphene FZP lens array under a reflection mode dark field optical microscopy: (a) optical image of the graphene FZP lens array. Each lenslet has twenty four zones and the radius of the centre zone is 10□m. (b) Graphene FZP showing the light focusing with excellent contrast. (c) Single FZP focusing spot. (d) Light intensity across the horizontal axis of the focal point in (c).

The lens arrays produced worked both in reflection and transmission mode of operation. In the transmission mode the focal point was produced within the glass substrate. Figure 5 shows the magnified version of a single graphene lens and focal points for two modes of operation. In figure 5(a), the dark zones are glass and the bright zones are graphene, which shows the good reflection optical contrast of few layer graphene on glass. By adjusting the focusing position of microscopy, we could get focusing spots both in glass (as show in figure 5(b), transmission mode) and in air (as show in figure 5(c), reflection mode).

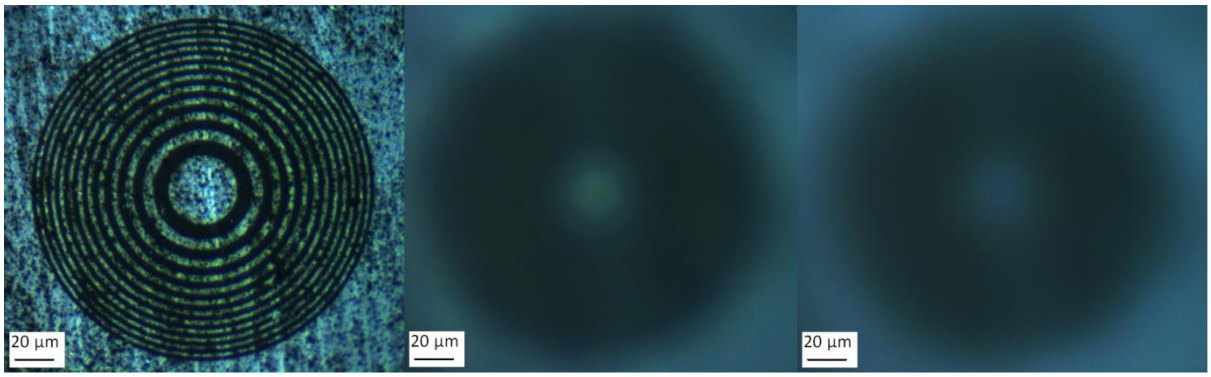

(a) (b) (c)

Figure 5. A single graphene FZP lenslet zoomed under optical microscope. (a) Magnified single graphene lenslet. (b) Graphene lens work as a transmission lens. (c) Graphene lens work as a reflection lens

To study the surface profile of the multi-layered graphene lens studies were carried out in atomic force microscope (AFM). AFM image of a single graphene FZP is shown in figure 6. The bright spots in figure 6(a) arise from the polymer residue post lithography and lead to artefacts in AFM images i.e. the black lines in figure 6(a). Figure 6(b) shows the information of the height distribution along the blue line. The Fresnel zones were clearly visible in the surface profile and the average surface roughness was measured as 3.47nm, which corresponds to approximately 10 layers of graphene. A few peaks in the range of 8-10 nm range are observed due to the left over polymer residues.

Optical transmission measurements were also performed for the multilayer graphene which was used for making the FZPs. An ocean optic spectrometer connected to the optical microscope was used to measure the transmission spectra. Transmission spectra for glass and graphene on glass were measured as shown in figure 6(c). The results show that compared to the bare glass substrate, graphene sample transmitted about 75-78% of the incident light. Theoretically, the transmission of 10 layer graphene is given by: $T \approx 1 - N\pi\alpha \approx 77\%$. So the measured data is in good agreement with the theoretical calculation.

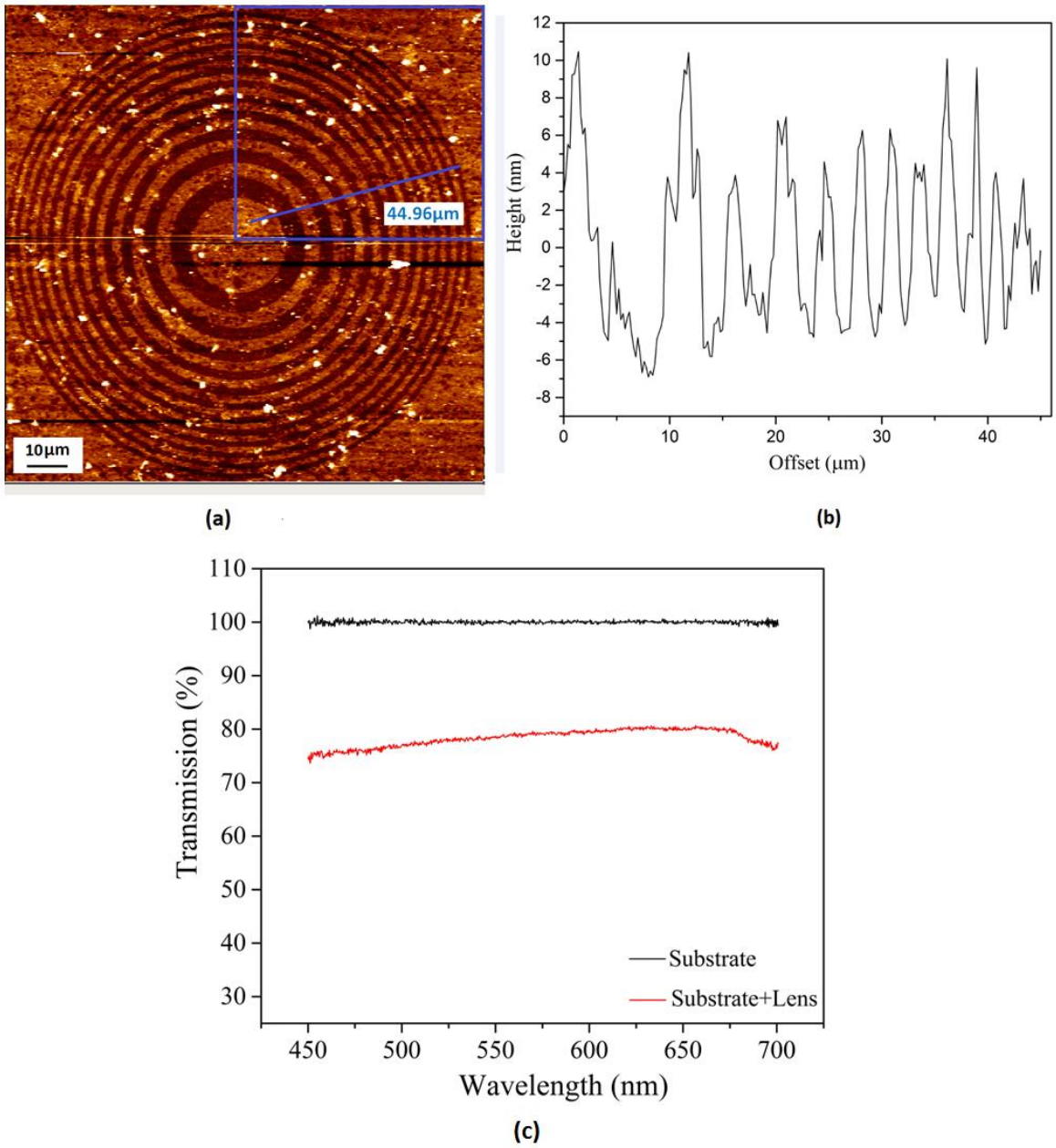

Figure 6. (a) AFM image of single graphene FZP. (b) Roughness distribution along the blue line. (c) Transmission spectrum for multi-layered graphene used for producing the lens array.

Finally to demonstrate the thinnest possible lens a single layer of graphene was used. Samples consisting of monolayer graphene were patterned lithographically onto 0.7 mm thick glass using a Microtech Laser writer (LW405, minimum resolution 0.7 µm) with a 405 nm laser. A positive resist (AZ5214) was used as an etch mask, spin coated at 4000 rpm and dried at 100^{o}C for 1 minute, resulting in a 1 µm thick resist film which was subsequently patterned with the laser and developed. The sample was then ashed under oxygen plasma (100 W, 5-10 minutes) to etch the exposed graphene layers, and subsequently washed thoroughly in acetone and 2-propanol to remove the remaining masking resist, leaving the patterned graphene surface. Figure 7(a) shows the single layered graphene FZP lens under optical microscope; while figures 7(e) and (g) demonstrate the same producing a focal point in the transmission and reflection modes of operation, respectively. The intensity profiles were also calculated across the focal points which demonstrate good contrast. The diffraction efficiency was measured to be around 4.1% for the transmission mode and 4.61% for the reflection mode.

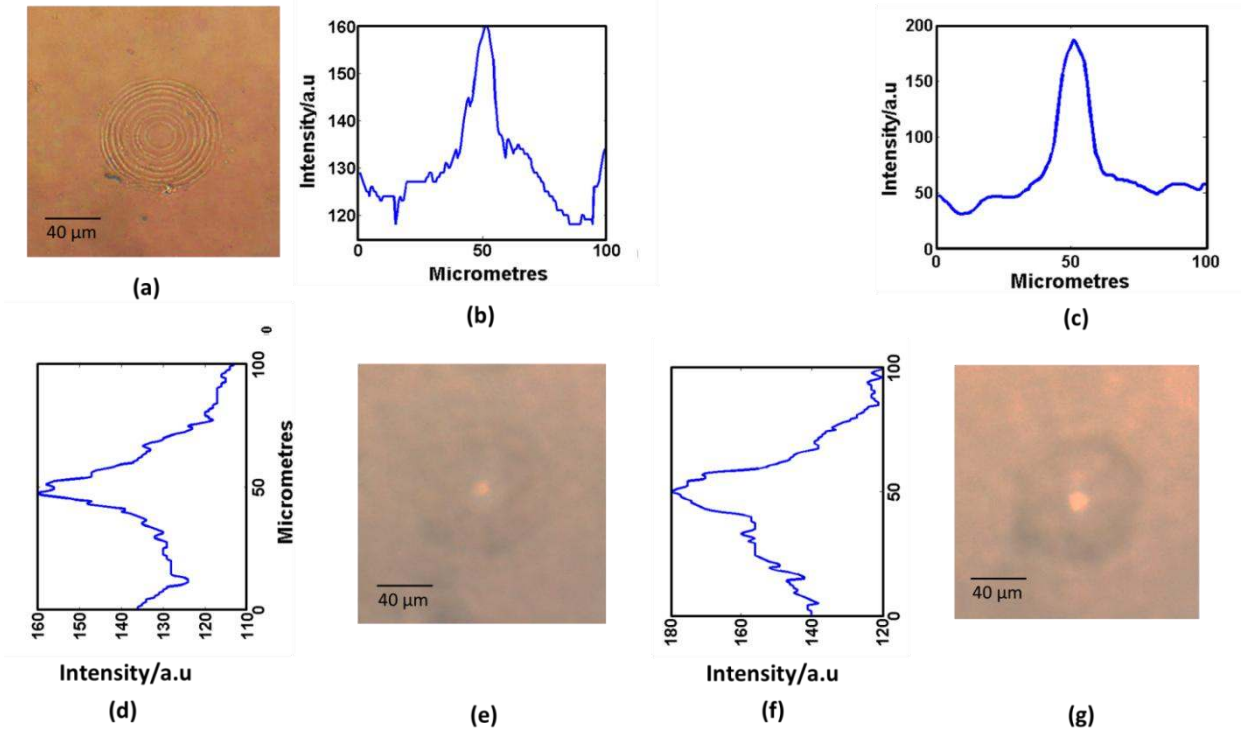

Figure 7. (a) Single layer graphene Fresnel zone plate zoomed under optical microscope. (e) and (g) show the lens working under transmission mode and reflection mode, respectively. (b) and (c) show the light intensity plots across the horizontal axis of transmission mode and reflection mode. (d) and (f) show the light intensity plots across the vertical axis of transmission mode and reflection mode focal point.

Producing the thinnest possible flat lens using the novel graphene material is a next step towards achieving high resolution, low noise and compact lenses for applications imaging applications. By increasing the widths of graphene based lens very high numerical apertures can also be achieved. Graphene is also being proposed as a transparent electrode for solar cells. By pattering it into the Fresnel zone plates-like geometries we demonstrated it can be simultaneously used as optical concentrator.

Moreover, as a future work graphene-based flat and compact lenses will be very useful in the terahertz range. In the terahertz frequency range, the conductivity (absorption) of graphene changes significantly with the Fermi level.[14, 27] Hence, by controlling the Fermi levels (electronically) the performance of graphene based lenses could be tuned. Figure 8 shows the simulation results carried out for the graphene based Fresnel zone plates operating at a wavelength of 10 µm. With the increase in wavelength of operation, the focal length of the lens has been reduced to just 10 µm in accordance with the Fresnel lens equation. Simulations were performed with different values of charge mobility and Fermi levels. As shown in figure 8(c), with an increase in the charge mobility no change in the intensity of the focused light is observed. However, the focal point intensity changes significantly with Fermi level of graphene for terahertz light illuminations. As shown in figure 8(d), that when the Fermi level is increased from 0.1 to 0.5eV the intensity of focal point increases by approximately two orders. Hence, we can expect an electrically tunable lensing effect using the graphene-based FZPs in the terahertz frequencies, which will be highly valuable for applications like terahertz imaging, detection and communications. Experimental verification of these simulation results will be done in future.

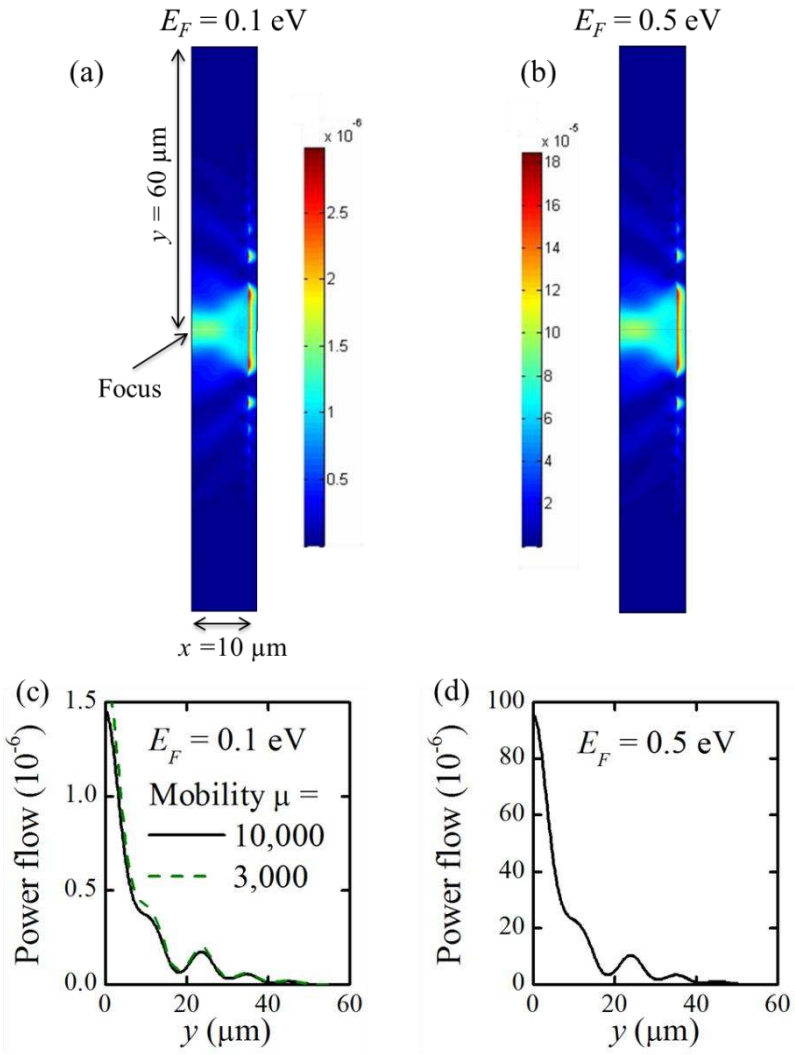

Figure 8. Power flow distributions of Fresnel zone plate made by 10-layer graphene for λ = 10 μm (i.e., light frequency equal to 30 THz) with Fermi level, E_F, being equal to (a) 0.1 and (b) 0.5 eV. The distribution across half of the focal plane for Fermi levels of (c) 0.1 and (d) 0.5 eV.

In conclusion, we have developed ultrathin multi and single-layer graphene-based Fresnel zone plate lenses on glass with nanoscale roughness. Through calculation and FEM computational modelling, the lenses were designed to operate in the optical regime. The lenses were fabricated by a lithography technique, and their focusing properties were characterized. The lenses were found to be thinner, more efficient, and easier to fabricate compared to the metasurface based flat lenses. Hence the graphene lens arrays are highly promising as flat and ultrathin lenses as they have the potential to revolutionize the design of compact optical systems, such as laser focusing for optical storage and fibre-optic communication.

Corresponding Author
*h.butt@bham.ac.uk, Tel: +44 121 415 8623, Fax: +44 121 414 3958

Present Addresses
†School of Mechanical Engineering, University of Birmingham, Edgbaston, Birmingham B15 2TT, UK

Author Contributions
The manuscript was written through contributions of all authors. All authors have given approval to the final version of the manuscript. #These authors contributed equally.

Acknowledgements
HB would like to thank The Leverhulme Trust for the research funding.

References

1. Aničin, B.; Babović, V.; Davidović, D. *American Journal of Physics* **1989,** 57, 312.
2. Rastani, K.; Marrakchi, A.; Habiby, S. F.; Hubbard, W. M.; Gilchrist, H.; Nahory, R. E. *Applied Optics* **1991,** 30, (11), 1347-1354.
3. Ferstl, M.; Frisch, A.-M. *Journal of Modern Optics* **1996,** 43, (7), 1451-1462.
4. Kodate, K.; Tokunaga, E.; Tatuno, Y.; Chen, J.; Kamiya, T. *Applied Optics* **1990,** 29, (34), 5115-5119.
5. Fallahi, M.; Kasunic, K. J.; Penner, S.; Nordman, O.; Peyghambarian, N. *OPTICE* **1998,** 37, (4), 1169-1174.
6. Morgan, B.; Waits, C. M.; Krizmanic, J.; Ghodssi, R. *Microelectromechanical Systems, Journal of* **2004,** 13, (1), 113-120.
7. Carter, D. J. D.; Gil, D.; Menon, R.; Mondol, M. K.; Smith, H. I.; Anderson, E. H. *Journal of Vacuum Science & Technology B* **1999,** 17, (6), 3449-3452.
8. Perry, M.; Shannon, C.; Shults, E.; Boyd, R.; Britten, J.; Decker, D.; Shore, B. *Optics letters* **1995,** 20, (8), 940-942.
9. Menon, R.; Gil, D.; Smith, H. I. *JOSA A* **2006,** 23, (3), 567-571.
10. Hessler, T.; Rossi, M.; Kunz, R. E.; Gale, M. T. *Applied optics* **1998,** 37, (19), 4069-4079.
11. Aieta, F.; Genevet, P.; Kats, M. A.; Yu, N.; Blanchard, R.; Gaburro, Z.; Capasso, F. *Nano Lett* **2012,** 12, (9), 4932-4936.
12. Geim, A. K.; Novoselov, K. S. *Nat. Mater.* **2007,** 6, (3), 183-191.
13. Butt, H.; Kidambi, P. R.; Dlubak, B.; Montelongo, Y.; Palani, A.; Amaratunga, G. A.; Hofmann, S.; Wilkinson, T. D. *Advanced Optical Materials* **2013,** 1, (11), 869-874.
14. Degl'Innocenti, R.; Jessop, D. S.; Shah, Y. D.; Sibik, J.; Zeitler, J. A.; Kidambi, P. R.; Hofmann, S.; Beere, H. E.; Ritchie, D. *ACS nano* **2014**.
15. Bao, Q.; Loh, K. P. *ACS nano* **2012,** 6, (5), 3677-3694.
16. Cooper, D. R.; D'Anjou, B.; Ghattamaneni, N.; Harack, B.; Hilke, M.; Horth, A.; Majlis, N.; Massicotte, M.; Vandsburger, L.; Whiteway, E. *ISRN Condensed Matter Physics* **2012,** 2012.
17. Nair, R.; Blake, P.; Grigorenko, A.; Novoselov, K.; Booth, T.; Stauber, T.; Peres, N.; Geim, A. *Science* **2008,** 320, (5881), 1308-1308.
18. Skulason, H.; Gaskell, P.; Szkopek, T. *Nanotechnology* **2010,** 21, (29), 295709.
19. Fan, Y.-H.; Ren, H.; Wu, S.-T. *Opt. Express* **2003,** 11, (23), 3080-3086.
20. Vakil, A.; Engheta, N. *Science* **2011,** 332, (6035), 1291-1294.
21. Gusynin, V.; Sharapov, S.; Carbotte, J. *Journal of Physics: Condensed Matter* **2007,** 19, (2), 026222.
22. Kidambi, P. R.; Ducati, C.; Dlubak, B.; Gardiner, D.; Weatherup, R. S.; Martin, M.-B.; Seneor, P.; Coles, H.; Hofmann, S. *The Journal of Physical Chemistry C* **2012,** 116, (42), 22492-22501.
23. Palik, E. D., *Handbook of Optical Constants of Solids: Index*. Access Online via Elsevier: 1998; Vol. 3.
24. Kidambi, P. R.; Bayer, B. C.; Blume, R.; Wang, Z.-J.; Baehtz, C.; Weatherup, R. S.; Willinger, M.-G.; Schloegl, R.; Hofmann, S. *Nano Lett* **2013,** 13, (10), 4769-4778.
25. Kidambi, P. R.; Bayer, B. C.; Weatherup, R. S.; Ochs, R.; Ducati, C.; Szabó, D. V.; Hofmann, S. *physica status solidi (RRL)-Rapid Research Letters* **2011,** 5, (9), 341-343.
26. Xi, K.; Kidambi, P. R.; Chen, R.; Gao, C.; Peng, X.; Ducati, C.; Hofmann, S.; Kumar, R. V. *Nanoscale* **2014**.
27. Badhwar, S.; Sibik, J.; Kidambi, P. R.; Beere, H. E.; Zeitler, J. A.; Hofmann, S.; Ritchie, D. A. *Applied Physics Letters* **2013,** 103, (12), 121110.